FEBS Letters 580 (2006) 3211–3216

Signaling pathway of ginsenoside-Rg1 leading to nitric oxide production in endothelial cells

Kar Wah Leung[a,1], Yuen-Kit Cheng[b,1], Nai Ki Mak[a], Kelvin K.C. Chan[c], T.P. David Fan[d], Ricky N.S. Wong[a,c,*]

[a] *Department of Biology, Hong Kong Baptist University, Hong Kong*
[b] *Department of Chemistry, Hong Kong Baptist University, Hong Kong*
[c] *Research and Development Division, School of Chinese Medicine, Hong Kong Baptist University, Hong Kong*
[d] *Angiogenesis and TCM Laboratory, Department of Pharmacology, University of Cambridge, Cambridge, UK*

Received 27 February 2006; revised 10 April 2006; accepted 28 April 2006

Available online 4 May 2006

Edited by Robert Barouki

Abstract **We here provide definitive evidence that ginsenoside-Rg1, the pharmacologically active component of ginseng, is a functional ligand of the glucocorticoid receptor (GR) as determined by fluorescence polarization assay. Rg1 increased the phosphorylation of GR, phosphatidylinositol-3 kinase (PI3K), Akt/PKB and endothelial nitric oxide synthase (eNOS) leading to increase nitric oxide (NO) production in human umbilical vein endothelial cell. Rg1-induced eNOS phosphorylation and NO production were significantly reduced by RU486, LY294,002, or SH-6. Also, knockdown of GR completely eliminated the Rg1-induced NO production. This study revealed that Rg1 can indeed serve as an agonist ligand for GR and the activated GR can induce rapid NO production from eNOS via the non-transcriptional PI3K/Akt pathway.**

Keywords: Ginsenoside-Rg1; Glucocorticoid receptor; Nitric oxide; Endothelial cells

1. Introduction

Panax Ginseng C.A. Meyer and its related species have been used as health tonics for centuries in Chinese medication. Ginsenosides, the pharmacologically active components found in ginseng, are triterpenoid saponins that are broadly classified into 20(*S*)-protopanaxatriols (PPT) and 20(*S*)-protopanaxadiols (PPD) [1]. Ginsenoside-Rg1, a PPT (see Fig. 5A), has been demonstrated to trigger transcriptional activation of a glucocorticoid responsive element (GRE)-containing reporter gene, suggesting that Rg1 can activate the glucocorticoid receptor (GR) [2]. Recently, glucocorticoids (GCs) have been reported to activate the phosphatidylinositol-3 kinase (PI3K)/Akt pathway after binding to the GR [3]. PI3K/Akt pathway is a crucial regulator in cell proliferation, cell-cycle progression, and a mediator of cellular survival [4]. The activated PI3K/Akt pathway leads to phosphorylation of endothelial nitric oxide synthase (eNOS) and increases the production of nitric oxide (NO) [5]. NO-related endothelial proliferation and angiogenesis were shown to be part of the activities of Rg1 [6]. To elucidate the role of the GR in Rg1-induced NO production, we have examined the state of GR activation and the downstream activation pathways of PI3K, Akt/protein kinase B (PKB) and eNOS in human umbilical vein endothelial cells (HUVEC). In addition, a molecular docking study of Rg1 to the GR was also performed. This work can provide molecular basis for the diverse activities of ginseng.

2. Materials and methods

2.1. Materials

Culture medium M199 and endothelial cell growth supplement (ECGS) were purchased from Sigma. Foetal bovine serum (FBS) was from Gibco. RU486, LY294,002 and ICI182,780 were from Sigma. SH-6 and L-NMMA was from Calbiochem and Cayman, respectively. Anti-GRα was from Santa Cruz Biotechnology. Anti-phospho-GR (Ser211) and anti-phospho-PI3 kinase p85 were from Cell Signaling. Anti-PI3 kinase p85, anti-Akt1/PKBα, anti-phospho-Akt1/PKBα (Ser473), anti-eNOS/NOSIII and anti-phospho-eNOS (Ser1177) were from Upstate. Anti-β-actin was from Sigma. Alexa Fluor 488 anti-rabbit IgG (Molecular Probe) and anti-rabbit IgG HRP (Zymed) were used for immunocytochemistry and immunoblotting, respectively. Small interfering RNA (siRNA) was custom-designed and purchased from Dharmacon (M-003424-02).

2.2. HUVEC culture conditions

HUVEC (Clonetics) were grown in M199 supplemented with 20% FBS, 20 μg/ml ECGS, 90 U/ml Heparin (Sigma), 1% penicillin–streptomycin–neomycin (PSN, Gibco) and 50 ng/ml amphotericin B (Sigma). Cultures were maintained at 37 °C in humidified CO_2 incubator (5% CO_2). HUVEC were used at passages 2–8.

2.3. NO production assay

HUVEC were seeded in a 96-well plate at 2×10^4 cells/well. Rg1 of various concentrations was prepared in serum-free medium. The concentrations of NO_2^- and NO_3^- in the culture medium were measured with the NO Detection Kit (Assay Design Inc.) by monitoring the optical density at 540 nm spectrophotometrically (iEMS analyzer, Labsystems). HUVEC were incubated with different concentrations of Rg1 at 37 °C for indicated treatment intervals. HUVEC were also pre-incubated with various antagonists/inhibitors: 10 μM RU486, 10 μM LY294,002, 20 μM SH-6, and 20 μM L-NMMA, respectively, each

*Corresponding author. Fax: +852 3411 5995.
E-mail address: rnswong@hkbu.edu.hk (R.N.S. Wong).

[1] These authors contributed equally to this work.

Abbreviations: GR, glucocorticoid receptor; GC, glucocorticoid; GRE, glucocorticoid responsive element; Dex, dexamethasone; eNOS, endothelial nitric oxide synthase; NO, nitric oxide; HUVEC, human umbilical vein endothelial cell; PI3K, phosphatidylinositol-3 kinase; PKB, protein kinase B; NR, nuclear receptor; LBD, ligand-binding domain

0014-5793/$32.00
doi:10.1016/j.febslet.2006.04.080

for 30 min with or without 150 nM Rg1 at 37 °C. Dexamethasone (Dex) (500 nM) acted as positive control. Concentrations of NO produced were calculated according to the calibration curve in each experiment and expressed as nanomoles per microgram protein (±standard deviation (S.D.)).

2.4. siRNA transfection

siRNA duplex oligo targeting GR mRNA was transfected with siLenfect (Invitrogen) at 5 nM into HUVEC. Concentrations of NO produced after 30 min treatment of Rg1 (150 nM) or Dex (500 nM) were estimated according to the method mentioned above.

2.5. Western blot analysis

Total cellular protein was obtained by lysing cells with lysis buffer (Novagen) supplemented with phosphatase and protease inhibitor cocktail (Merck). SDS–PAGE resolved protein bands were transferred to nitrocellulose membranes (Amersham). After blocking with 5% skimmed milk, the membrane was incubated with primary antibodies (1:1000 dilution) for 3 h, followed by horseradish peroxidase-conjugated IgG (1:2000 dilution). Target proteins were visualized with enhanced chemiluminescence reagents (BioRad). Semi-quantifications were performed with densitometric analysis by Metamorph software.

2.6. GR competitive ligand-binding assays

Commercially available GR competitive binding assay was used (Invitrogen). Serial 2-fold dilution of Dex (1 μM to 0.9 nM) and Rg1 (2 μM to 1.8 nM) were competed with Fluormone, a proprietary fluorescent GC ligand provided in the kit, for binding to the human GR. The fluorescence polarization was measured by a PTI Fluorescence Lifetime Scanning Spectrometer. Negative (without any ligand; 0% competition) and positive (1 mM Dex; 100% competition) controls delimited the fluorescence polarization range. IC_{50} is defined as the concentration of a test compound that causes a half-maximum shift in polarization. The equilibrium dissociation constant (K_d) is the concentration of the competing ligand occupying half of the binding sites in the absence of the tracer ligand. The equilibrium binding curves were fitted with a two-state one-site competition model.

2.7. Translocation of phosphorylated GR

Images of the phosphorylated GR in HUVEC were collected with a Zeiss LSM-510 multi-tracking laser scanning confocal microscope (Carl Zeiss SAS, Frankfurt, Germany) for translocation study. HUVEC (5×10^4 cells) seeded on 13-mm diameter coverslips were fixed with 4% paraformaldehyde and incubated in anti-phospho-GR (Ser211) antibody with 0.1% Triton X-100 (Chemicon) and 2% normal goat serum (Gibco) for 3 h, followed by incubating in Alexa Fluor 488 in dark for 2 h. The coverslips were mounted with DAKO mounting medium. Images were captured (63×) within 72 h. For each treatment, 50 cells were analyzed and the ratio of nucleus/cytoplasm fluorescence intensity ($R_{N/C}$) was calculated.

2.8. Statistical analysis

Numerical results were analyzed using one-way ANOVA with Duncan post hoc test. Values shown are means of at least $N = 3$ experiments with ±S.D. Differences were considered statistically significant at a value of $P \leqslant 0.05$. Data significantly different from control was marked with * in the figures.

3. Results

3.1. Rg1 increases NO production

The production of NO by HUVEC was increased by treatment with Rg1 over a 15-fold dose range (Fig. 1A). Based on this finding, HUVEC were challenged with 150 nM Rg1 and the time profile of NO production was monitored for 60 min. An immediate linear rise in the total NO level was detected followed by a plateau after 10 min (Fig. 1B). Using Western blotting, the phosphorylation of eNOS at Ser1177 in response to Rg1 treatment was detected. An approximately 2.5-fold increase in the phosphorylated form of eNOS was detected as early as 10 min and this trend continued to increase up to 60 min after the exposure of HUVEC to 150 nM Rg1 (Fig. 2A). This provides direct evidence that Rg1 rapidly activates eNOS in HUVEC.

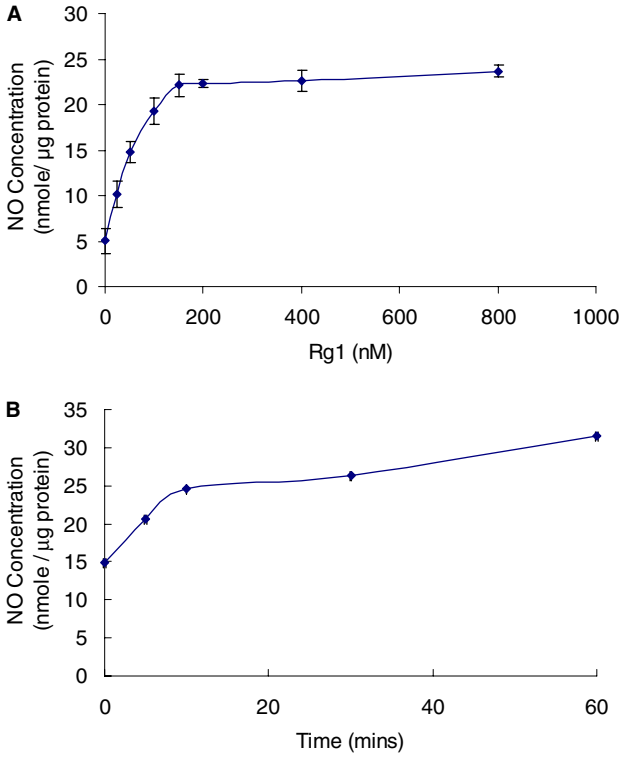

Fig. 1. Induction of NO production in HUVEC. (A) Cells were treated with a 15-fold range of Rg1 concentration for 60 min. (B) The time profile of NO production after 150 nM Rg1 treatment. The activity of NOS was quantified by measuring NO_2^- and NO_3^- concentrations in serum-free culture media. Total NO production was calculated from a calibration curve generated from standards provided by the manufacturer and normalized by the protein content of the corresponding wells ($N = 3$; ±S.D.). All data were significantly different from control at a value of $P \leqslant 0.05$.

3.2. Activation of eNOS via the GR and PI3K/Akt pathway

The upstream phosphorylation of the GR (Ser211), PI3K p85-subunit and Akt/PKB (Ser473) were also found to increase during the 60 min duration of exposure to 150 nM Rg1 as determined by Western blotting (Fig. 2B). The phosphorylation of GR was peaked at 10 min and dropped back to the base level at 60 min. The phosphorylation of PI3K and Akt/PKB, however, were more sustainable after reaching their maximum at 15 and 30 min, respectively. These results indicated a sequential activation from the GR to the PI3K/Akt pathway. The Rg1-induced eNOS phosphorylation at Ser1177 was abolished by the GR antagonist RU486; PI3K inhibitor LY294,002; and Akt/PKB inhibitor SH-6 (Fig. 3). Also, the production of NO was diminished to the baseline level in the presence of RU486 (Fig. 4). However, the Rg1-induced NO production was unaffected by an estrogen receptor (ER) antagonist ICI182,780 (10 μM) (Fig. 4),. Moreover, knockdown of the GR by siRNA completely eliminated the Rg1-induced NO production (Fig. 4).

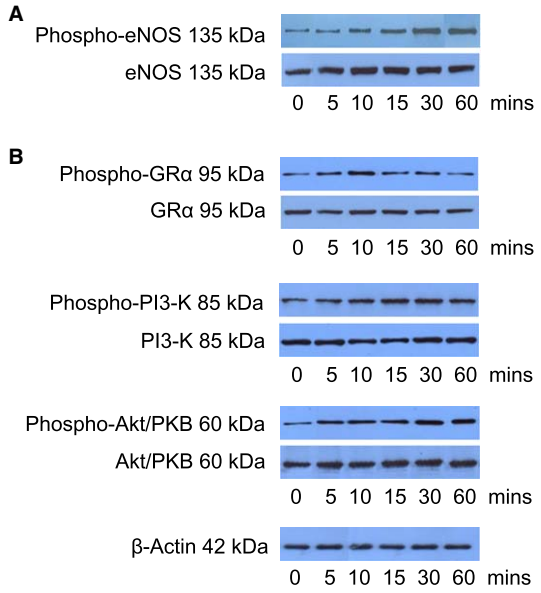

Fig. 2. Phosphorylation of signaling molecules after treatment with Rg1 over a time frame of 60 min. (A) Phosphorylated eNOS (Ser1177) detected by specific antibody was increased after 150 nM Rg1 treatment, while total eNOS had no change in quantity. (B) Phosphorylated forms of GRα (Ser211), PI3K and Akt/PKB (Ser473) were also found to increase after treatment with 150 nM Rg1 with no change in the respective total form. Protein loading was normalized by β-actin.

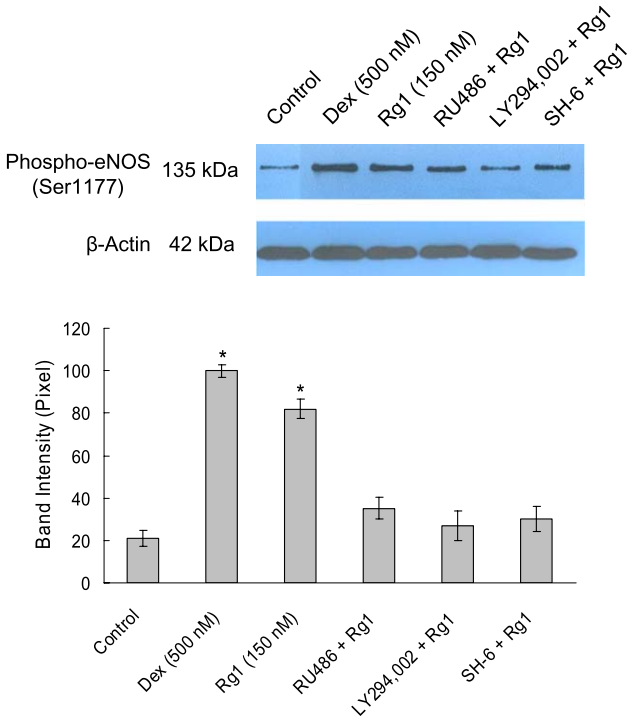

Fig. 3. Inhibition of eNOS phosphorylation at Ser1177 with different inhibitors/antagonists of the PI3K/Akt pathway. HUVEC pre-treated with indicated inhibitors/antagonists for 30 min were incubated with Rg1 (150 nM) for another 30 min. The phosphorylated form of eNOS (Ser1177) was greatly reduced in the presence of inhibitors/ antagonists. Protein loading was normalized by β-actin ($N = 3$; ± S.D.).

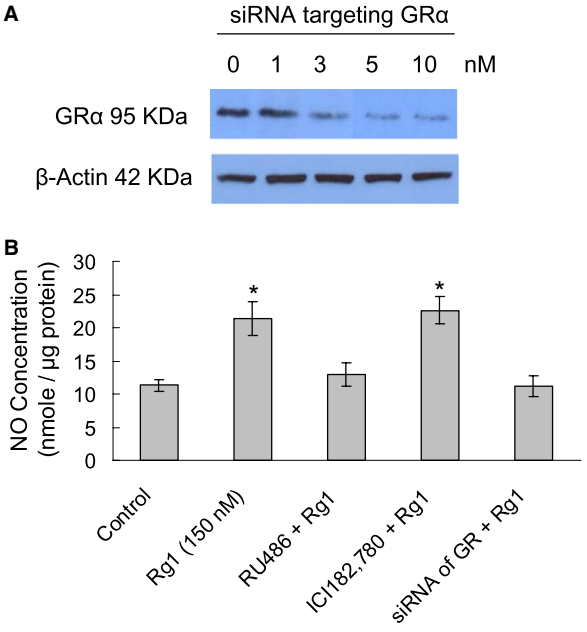

Fig. 4. Inhibition of NO production by steroid receptor antagonists. (A) Efficacy of the siRNA targeting GRα with protein loading normalized by β-actin. (B) HUVEC pre-treated with RU486 (10 μM) or ICI182,780 (10 μM) for 30 min were incubated with Rg1 (150 nM) for another 30 min. RU486, but not ICI182,780, suppressed the NO production back to the basal level. Also, GRα knockdown inhibited the Rg1-induced NO production. Total NO production was calculated from a calibration curve of standards provided by the manufacturer and normalized by the protein content of the corresponding wells ($N = 5$; ±S.D.).

3.3. Rg1 binding to the GR

A competitive ligand-binding assay was performed to study the specific binding of Rg1 to the GR using a proprietary fluorescent GC ligand (Fluormone)-recombinant human GR complex. Displacement of Fluormone from the GR-Fluormone complex by Rg1 results in a decrease in fluorescence polarization. The shift in polarization is used to determine the relative specific affinity of that ligand for the GR. The competitive ligand-binding assay indicated that Rg1 is indeed a ligand of the GR (Fig. 5A). The K_d values for Dex and Rg1 were 3.35 nM (IC_{50}, 10.55 nM; $R^2 = 0.99$) and 39.40 nM (IC_{50}, 128.50 nM; $R^2 = 0.98$), respectively (Fig. 5A). We speculated that Rg1 may bind to the same site as of Dex that is the ligand-binding domain (LBD) of the GR. Using the crystal structure of GR–LBD and Dex, we were able to show by modeling the docking of Rg1 to the ligand-binding site in place of Dex (Fig. 5B). Although the attached glucosyl rings on Rg1 cause steric bumps, this ginsenoside molecule still marginally fits into the hydrophobic cavity around the LBD even without significant conformational rearrangement of the protein.

3.4. Translocation of the phosphorylated GR

Ligand-activated steroid receptors can elicit both rapid non-transcriptional and genomic effects. The genomic effects of Rg1 binding to the GR were assessed by monitoring the translocation of the GR-ligand complexes from cytoplasm to nucleus. Exposure of HUVEC to Rg1 (150 nM) and Dex (5 μM) resulted in almost 2- and 5-fold increase in the ratio of nuclear/cytoplasmic fluorescent intensity ($R_{N/C}$), respectively

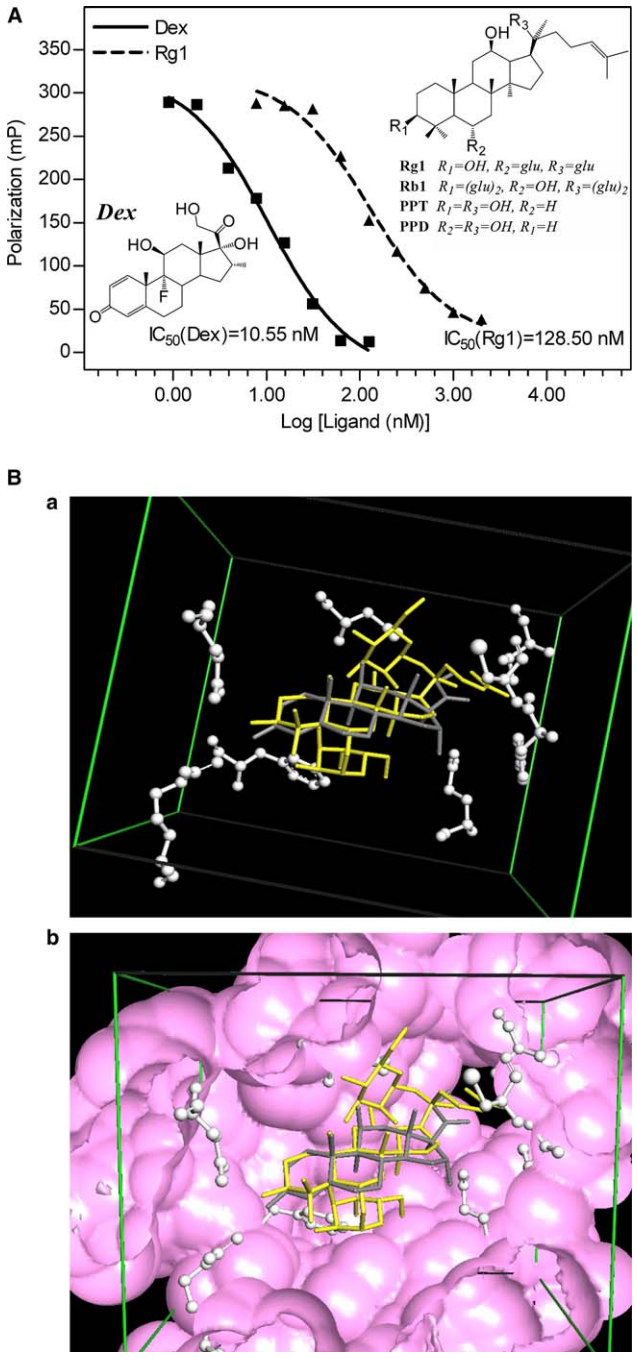

Fig. 5. (A) The GR-binding assays of Dex and the ginsenoside-Rg1 shown with their structures. The *Y*-axis is the fluorescence polarization (mP). For the ginsenosides, the glucosyl groups are abbreviated as "glu". The fitted curves are assumed to be one-site competition ($N = 3$). (B) The ginsenoside-Rg1 (yellow) preliminarily docked to the GR–LBD (molecule 1 of PDB:1P93, [28]) co-crystallized in the presence of Dex (grey) using ArgusLab [29]. The green cubic box shown is the region for defining the binding site of the receptor for docking. The agonistic ligand-binding residues in the LBD (clockwise from the top left: Q570, N564, C736, T739, Q642, F623, R611) are rendered in ball-and-stick (white). (a) Only with the ligand-binding residues shown. (b) The solvent accessible surface (probe radius = 1.4 Å) of the protein is included (pink). The docking residues defined in the green box for docking were excluded in creating the surface for clarity.

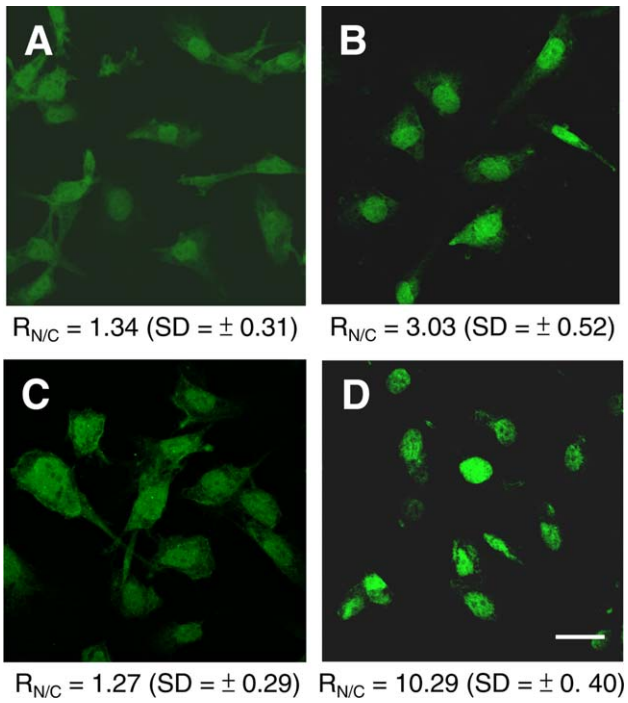

Fig. 6. Translocation of the phosphorylated GRα (Ser211) after treatment with Rg1. Treated HUVEC immunostained with anti-phospho-GR (Ser211). The images were captured by confocal microscope (63×) with identical settings. $R_{N/C}$, the ratio of nuclear/cytoplasmic fluorescent intensity of 50 cells from each treatment was calculated. (A) Negative control. (B) 150 nM Rg1 for 30 min. (C) HUVEC pre-treated with 10 μM RU486 for 30 min, then co-treated with 150 nM Rg1 for another 30 min. (D) 5 μM Dex for 30 min. The micrographs showed that the GR was phosphorylated and translocated into the nucleus in the presence of Rg1 or Dex, while the translocation was abolished by pretreatment with RU486. Scale bar = 20 μm.

(Fig. 6). This indicated that both Rg1 and Dex not only enhance the phosphorylation of the GR, but also induce the translocation of the phosphorylated GR into the nucleus. Furthermore, the translocation due to Rg1 was inhibited by the GR-antagonist RU486 (Fig. 6C). That means the blockade of the GR by RU486 not only affects the non-transcriptional pathways of Rg1, but also the transcriptional ones.

4. Discussion

GCs are a class of stress-induced steroid hormones that exert their actions through activation of GR, a member of the nuclear receptor (NR) superfamily [7]. Increasing evidence shows that activation of the GR triggers non-transcriptional pathways that lead to NO production and vasodilation within minutes [8]. Clinically, for patients with myocardial infarction [9,10] and ischaemic stroke [11], high doses of corticosteroids or Dex were given to activate eNOS and subsequently induce vasodilation to transiently decrease blood pressure and systemic vascular resistance accompanied by an increase in coronary and cerebral blood flow [9–11]. The current findings provide direct evidence that the Rg1 exerts GC-like effects by acting as a functional ligand of the GR to induce non-transcriptional effect leading to NO production through PI3K/Akt pathway in endothelial cells.

The eNOS is one of the isoforms of the NOS family responsible for NO production in HUVEC [12]. NO is an important transcellular signaling molecule contributing to anti-tumor [13], anti-microbial [14], anti-inflammatory [15], anti-oxidative [16] and immunosuppressive activity of macrophages [14–16]. Owing to its vasodilating property, NO plays an important role in cardiovascular protection [17]. The increased phosphorylation of eNOS (Ser1177) and NO production in HUVEC after exposure to Rg1 indicated that part of the physiological effects of Rg1 could be mediated by NO.

Western blot analysis indicated that Rg1 can rapidly activate GR, PI3K and Akt/PKB. The PI3K/Akt pathway is known as one of the candidates that are capable of activating eNOS directly [18]. In the present study, phosphorylation of eNOS and NO production were abolished by the inhibitors/antagonists: RU486 [19], LY294,002 [20], or SH-6 [21], whilst ICI182,780 had no effect. Since RU486 can act as a progesterone receptor (PR) antagonist [22], siRNA targeting GR was used in HUVEC in order to preclude the involvement of other NRs in the Rg1 induction pathway. Our results showed GR knockdown completely abolished the Rg1-induced NO production. These data confirmed the predominant involvement of GR and the PI3K/Akt pathway in the Rg1-induction pathway, while the ER and PR were not involved.

The activated PI3K phosphorylates phosphatidylinositol-4,5-bisphosphate (PIP_2), resulting in phosphatidylinositol-3,4,5-triphosphate (PIP_3) that subsequently binds to Akt/protein kinase B (Akt/PKB) [23]. Activation of PI3K/Akt pathway is a key step for diverse biological effects, including cell proliferation, growth, and survival [24,25]. Therefore, cellular activities brought about by the Rg1-activated PI3K/Akt pathway via the specific binding with the GR warrant further investigations. The present results showed that Rg1 is able to trigger the rapid non-transcriptional effects through the GR → PI3K → Akt/PKB → eNOS.

Upon ligand binding, the GR dissociates from hsp90-based chaperones, translocates from cytoplasm to nucleus and regulates gene expression by complexing with the GRE [26,27]. We demonstrated that the translocation of the phospho-GR in HUVEC was enhanced by Rg1 and Dex by immunofluorescence study. The competitive binding assay and the molecular docking study support the view that Rg1 can exert its genomic effects by binding to the LBD of the GR.

In view of the steroidal skeleton of the ginsenosides and the similarity of the side effects of ginseng overdosing to those of the corticosteroids or estrogens, the hypothesis that ginsenosides can act as steroid hormones is sustainable. In the present study, we have clearly demonstrated that Rg1 can act as an agonist for the GR, leading to transcriptional and non-transcriptional effects. However, Rg1 represents only one of the major ginsenosides in ginseng, the study of the combinatorial interactions between ginsenosides and the diverse NRs and their effects will be an important step towards unraveling the mystery of ginseng.

Acknowledgement: The present work was supported by an Earmarked Research Grant (HKBU 2171/03M) of the Research Grant Council, Hong Kong SAR Government.

References

[1] Liu, Z.Q., Luo, X.Y., Liu, G.Z., Chen, Y.P., Wang, Z.C. and Sun, Y.X. (2003) In vitro study of the relationship between the structure of ginsenoside and its antioxidative or prooxidative activity in free radical induced hemolysis of human erythrocytes. J. Agric. Food Chem. 51, 25555–25558.
[2] Lee, Y.J., Chung, E., Lee, K.Y., Lee, Y.H., Huh, B. and Lee, S.K. (1997) Ginsenoside-Rg1, one of the major active molecules from Panax ginseng, is a functional ligand of glucocorticoid receptor. Mol. Cell. Endocrinol. 133, 135–140.
[3] Dancey, J.E. (2004) Molecular targeting: PI3 kinase pathway. Ann. Oncol. 15 (Suppl. 4), 233–239.
[4] Vivanco, I. and Sawyers, C.L. (2002) The phosphatidylinositol 3-kinase AKT pathway in human cancer. Nature 2, 489–501.
[5] Nathan, C. and Xie, Q.W. (1994) Nitric oxide synthases: roles, tolls, and controls. Cell 78, 915–918.
[6] Knowles, R.G. and Moncada, S. (1994) Nitric oxide synthases in mammals. Biochem. J. 298, 249–258.
[7] Tache, J. and Selye, H. (1985) On stress and coping mechanisms. Issues Ment. Health Nurs. 7, 3–24.
[8] Limbourg, F.P. and Liao, J.K. (2003) Nontranscriptional actions of the glucocorticoid receptor. J. Mol. Med. 81, 168–174.
[9] Libby, P., Maroko, P.R., Bloor, C.M., Sobel, B.E. and Braunwald, E. (1973) Reduction of experimental myocardial infarct size by corticosteroid administration. J. Clin. Invest. 52, 599–607.
[10] Yanagisawa-Miwa, A., Uchida, Y., Nakamura, F., Tomaru, T., Kido, H., Kamijo, T., Sugimyo, T., Kajji, K., Utsuyama, M. and Kurashima, C. (1992) Salvage of infarcted myocardium by angiogenic action of basic fibroblast growth factor. Science 257, 1401–1403.
[11] Limbourg, F.P., Huang, Z., Plumier, J., Simoneini, T., Fujioka, M., Tuckermann, J., Schutz, G., Moskowitz, M.A. and Liao, J. (2002) Rapid nontranscriptional activation of endothelial nitric oxide synthase mediates increased cerebral blood flow and stroke protection by corticosteroids. J. Clin. Invest. 110, 1729–1738.
[12] de Assis, C.M., Plotkowski, C.M., Fierro, I.M., Barja-Fidalgo, C. and de Freitas, M.S. (2002) Expression of inducible nitric oxide synthase in human umbilical vein endothelial cells during primary culture. Nitric Oxide 7, 254–261.
[13] Sun, H., Gutierrez, P., Jackson, M.J., Kundu, N. and Fulton, A.M. (2000) Essential role of nitric oxide and interferon-gamma for tumor immunotherapy with interleukin-10. J. Immunother. 23, 208–214.
[14] Fang, F.C. (1997) Perspectives series: host/pathogen interactions. Mechanisms of nitric oxide-related antimicrobial activity. J. Clin. Invest. 99, 2818–2825.
[15] Miyataka, M., Rich, K.A., Ingram, M., Yamamoto, T. and Bing, R.J. (2002) Nitric oxide, anti-inflammatory drugs on renal prostaglandins and cyclooxygenase-2. Hypertension 39, 785–789.
[16] Mohanakumar, K.P., Thomas, B., Sharma, S.M., Muralikrishnan, D., Chowdhury, R. and Chiueh, C.C. (2002) Nitric oxide: an antioxidant and neuroprotector. Ann. NY Acad. Sci. 962, 389–401.
[17] Sengupta, S., Toh, S.A., Sellers, L.A., Skepper, J.N., Koolwijk, P., Leung, H.W., Yeung, H.W., Wong, R.N.S., Sasisekharan, R. and Fan, D.T.P. (2004) Modulating angiogenesis: the yin and the yang in ginseng. Circulation 110, 1219–1225.
[18] Isenovic, E.R., Meng, Y., Divald, A., Milivojevic, N. and Sowers, J.R. (2002) Role of phosphatidylinositol 3-kinase/Akt pathway in angiotensin II and insulin-like growth factor-1 modulation of nitric oxide synthase in vascular smooth muscle cells. Endocrine 19, 287–292.
[19] Collins, P.W. (1990) Misoprostol: discovery, development, and clinical applications. Med. Res. Rev. 10, 149–172.
[20] Vlahos, C.J., Matter, W.F. and Hui, K.Y. (1994) A specific inhibitor of phosphatidylinositol 3-kinase, 2-(4-morpholinyl)-8-phenyl-4H-1-benzopyran-4-one (LY294,002). J. Biol. Chem. 269, 5241–5248.
[21] Kozikowski, A.P., Sun, H., Brognard, J. and Dennis, P.A. (2003) Novel PI analogues selectively block activation of the pro-survival serine/threonine kinase Akt. J. Am. Chem. Soc. 125, 1144–1145.
[22] Bardon, S., Vignon, F., Chalbos, D. and Rochefort, H.J. (1985) RU486, a progestin and glucocorticoid antagonist, inhibits the growth of breast cancer cells via the progesterone receptor. Clin. Endocrinol. Metab. 60, 692–697.
[23] Czech, M.P. (2000) PIP2 and PIP3: complex roles at the cell surface. Cell 100, 603–606.

[24] Dimmeler, S., Fleming, I., Fisslthaler, B., Hermann, C., Busse, R. and Zeiher, A.M. (1999) Activation of nitric oxide synthase in endothelial cells by Akt-dependent phosphorylation. Nature 399, 601–605.
[25] Huang, H.N., Lu, P.J., Lo, W.C., Lin, C.H., Hsiao, M. and Tseng, C.J. (2004) In situ Akt phosphorylation in the nucleus tractus solitarii is involved in central control of blood pressure and heart rate. Circulation 110, 2476–2483.
[26] Moran, T.J., Gray, S., Mikosz, C.A. and Conzen, S.D. (2000) The glucocorticoid receptor mediates a survival signal in human mammary epithelial cells. Cancer Res. 60, 867–887.
[27] Dostert, A. and Heinzel, T. (2004) Negative glucocorticoid receptor response elements and their role in glucocorticoid action. Curr. Pharm. 10, 2807–2816.
[28] Kauppi, B., Jakob, C., Farnegardh, M., Yang, J., Ahola, H., Alarcon, M., Calles, K., Engstrom, O., Harlan, J. and Muchmore, S. (2003) The three-dimensional structures of antagonistic and agonistic forms of the glucocorticoid receptor ligand-binding domain: RU-486 induces a transconformation that leads to active antagonism. J. Biol. Chem. 278, 22748–22754.
[29] Thompson, M.A. ArgusLab 4.0, Planaria Software LLC, Seattle, WA. Available from: <http://www.arguslab.com>.